

1 **Multi-objective optimization of organic Rankine cycle system for the waste heat**
2 **recovery in the heat pump assisted reactive dividing wall column**

3 Ao Yang ^a, Yang Su ^a, Weifeng Shen ^{a,*}, I-Lung Chien ^b, and Jingzheng Ren ^c

4 ^a School of Chemistry and Chemical Engineering, Chongqing University, Chongqing 400044,
5 People's Republic of China

6 ^b Department of Chemical Engineering, National Taiwan University, Taipei 10617, Taiwan

7 ^c Department of Industrial and Systems Engineering, Hong Kong Polytechnic University,
8 Hong Kong SAR, People's Republic of China

9 ***Corresponding author:** (W. S.) shenweifeng@cqu.edu.cn

10 **Abstract:** The application of heat pump (HP) technique to reactive dividing wall column
11 (RDWC) achieving energy-saving has received more and more attention, however, massive
12 low-temperature (<100 °C) waste heat would be hereby produced. Therefore, in this work, the
13 organic Rankine cycle (ORC) is adopted to effectively convert the produced waste heat of the
14 compressed stream to clean energy (i.e., electricity). The HP assisted RDWC (HP-RDWC) of
15 diethyl carbonate process is taken as an example, the ORC system with five working fluids
16 candidates are explored. The operating parameters of the ORC system (e.g., flow rate of
17 working fluid and inlet pressure of evaporator) are optimized based upon the maximum net
18 revenue and ORC thermal efficiency through the improved multi-objective genetic algorithm.
19 The optimal ORC system is determined by considering the economic (i.e., net revenue) and
20 thermodynamic efficiency (i.e., ORC efficiency) performances. The results illustrated that the
21 net revenue of the ORC system with R123 and R600a could achieve 175,807.2 US\$ and
22 133,665.5 US\$ with ORC efficiency of 15.57 and 16.19%. In addition, total annual cost of

23 the HP-RDWC integrated ORC processes with working fluids R123 and R600a could be
24 reduced by 11.78% and 10.30%, respectively.

25 **Keywords:** Energy conversion; Waste heat recovery; Clean energy; Organic Rankine cycle;
26 Multi-objective optimization

27 1. Introduction

28 Environmental protection and sustainable development could be achieved via the
29 effective utilization of the energy sources [1, 2]. A thermally-coupled technique, dividing wall
30 column (DWC), as a consequence is reported to reduce the fixed investment and utility
31 consumption by integrating two conventional columns into a single separation unit as proved
32 by Petlyuk et al. [3]. DWC is divided into four sections (a shared rectifying and stripping
33 sections, a pre-separation section, and a side draw section) via a divided-wall as shown in
34 Figure A1. The first commercialization of the DWC technology is implemented by BASF [4].
35 Subsequently, Benyounes et al. [5] explored the application of the DWC to separate
36 non-azeotropic mixtures. Seihoub et al. [6] studied the DWC for the liquefied petroleum gas
37 process. Long et al. [7] investigated a systematic optimization approach for separating ternary
38 mixtures benzene/toluene/*o*-xylene via the DWC configuration. The energy-saving of DWC
39 is further proved through retrofitting six industrial processes [8]. Following that, Kiss et al. [9]
40 proposed an energy-saving process to synthesize fatty acid methyl esters by combining
41 reaction with DWC (denoted as RDWC) and they illustrated that 25% savings of energy
42 consumption could be achieved. Yang et al. [10] reported a RDWC configuration to produce
43 gasoline additive tert-amyl methyl ether and they proved that the proposed RDWC process
44 can save 43.58% of total annual cost (TAC). At the same time, the synthesis of diethyl

45 carbonate is explored via the RDWC sequence and they demonstrated that the utility
46 consumption and TAC of the RDWC scheme could save 18.7% and 13.9% compared with
47 the conventional reactive distillation scheme [11]. The hydrolysis of methyl acetate through
48 the RDWC configuration is studied by Li et al. [12] and they displayed that 20.1% energy
49 savings can be achieved by the RDWC scheme. In summary, energy consumption and TAC
50 could be significantly reduced via the application of the DWC configuration, which is
51 applicable to ideal, azeotropic or reaction systems.

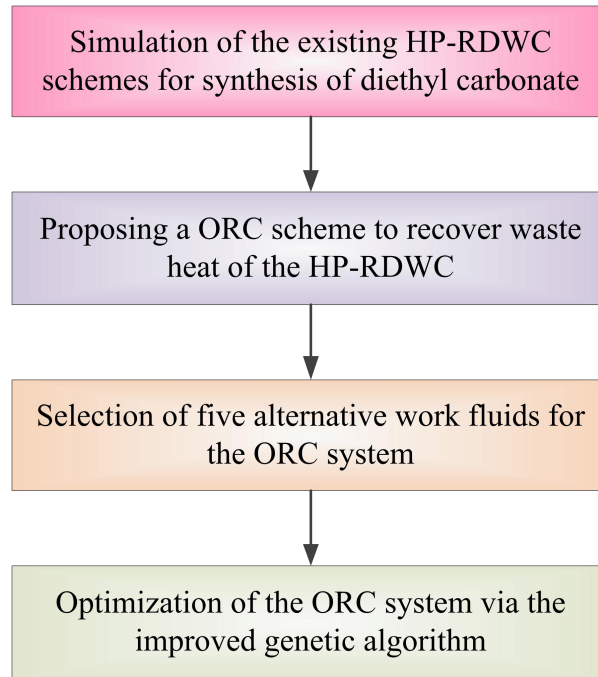
52 The RDWC configuration has a huge potential in decreasing both energy consumption
53 and TAC. Unfortunately, the latent heat of vaporization of the condensed vapor stream in the
54 condenser has not been fully used, as such, the heat pump (denoted as HP) technique is used
55 [13, 14]. For example, Feng et al. [15] explored a HP assisted RDWC (HP-RDWC) for the
56 synthesis of isopropyl acetate and the computational illustrated that the utility consumption
57 and TAC save 49.9% and 13.8%. An energy-efficient scheme for diethyl carbonate process
58 via the RDWC with different pressure thermally-coupled is investigated by Yang et al. [16]
59 and the result indicated that the significant reduction of TAC is achieved by 20.5%.
60 HP-RDWC configuration for production of *n*-amyl alcohol and *n*-hexanol is explored [17]
61 and the simulation displayed that the steam investment of the HP-RDWC could be reduced to
62 62.5% compared with the existing RDWC process. Feng et al. [18] proposed an
63 energy-saving HP-RDWC separation scheme for producing *n*-propyl acetate and the
64 calculation demonstrated that the TAC could be significantly reduced. In addition, the
65 HP-RDWC configuration for different process has been extensively studied by other
66 researchers [19, 20].

67 The utility consumption and TAC could be further reduced via the HP technique.
68 However, the major defects of the HP system are producing a massive low-temperature (<100
69 °C) waste heat, that is to say, energy of the compressed stream has not been effectively
70 utilized. To solve this issue, the organic Rankine cycle (ORC) technology is used to utilize
71 the waste heat [21]. ORC system is applied to the HP assisted distillation for separating
72 mixture benzene and toluene as reported by Gao et al. [22] and they illustrated that the TAC
73 can further decrease 6.47% compared with the HP scheme. Following that, the comparison
74 between conventional ORC and a preheater for evaporator ORC are studied [23] and they
75 proved that the electrical energy of the HP process can be reduced by 21.29%. Baccioli et al.
76 [24] investigated the waste heat recovery for the multi-effect distillation process via the ORC
77 system and they presented that the thermodynamic efficiency could be effectively improved.
78 Waste heat recovery of the liquefied natural gas is studied via a triple ORC scheme [25].
79 Hipólito-Valencia et al. [26] proposed an novel approach for waste heat recovery by
80 combining ORCs and heat exchanger network based on the proposed superstructure. Massive
81 waste heat of the bioethanol purification process is converted to produce clean energy via
82 ORC system and the results displayed that the application of ORC scheme yields significant
83 economic benefits [27]. Additionally, the waste heat in the other industries could be
84 recovered by using the ORC system [28-38]. A dual-loop ORC scheme is used to recover
85 waste heat for engine system [39]. Waste heat recovery of compact heat exchangers is
86 reported via the ORC system [40]. Li et al. [41] proposed a novel extractive distillation
87 process by combining economizer and ORC to effectively use the heat duty of condenser.
88 According to the above listed studies, the low-temperature waste heat could be effectively

89 recovered via the ORC system.

90 To the best of our knowledge, valuable insights on conceptual design and
91 multi-objective optimization by combining the ORC system to HP-RDWC system have not
92 yet been reported. In this contribution, we report a new diethyl carbonate (DEC) process
93 combining ORC to the HP-RDWC process. In this process, massive waste heat produced by
94 HP is effectively utilized to produce clean energy via ORC system. To obtain the best
95 performances of ORC system, five alternative dry working fluids involving R113, R123,
96 R245fa, R600a, and R601a are selected based on the temperature-entropy (T-S) diagram and
97 thermo-physical properties. An improved multi-objective genetic algorithm is adopted to
98 optimize the ORC system, which can reduce the repeated solutions and increase evolution
99 rate by adding a tournament & select best individuals step. In the optimization process, two
100 conflict objectives including net revenue and ORC thermal efficiency are determined. Finally,
101 two ORC systems are evaluated by considering the economic (i.e., net revenue) and
102 thermodynamic efficiency (ORC efficiency) performances.

103 **2. Methodology**



104

105 **Figure 1.** Proposed procedure for the waste heat recovery of the HP-RDWC process via the
 106 ORC system (HP-RDWC: heat pump assisted reactive dividing wall column; ORC: organic
 107 Rankine cycle)

108 A systematic approach for the waste heat recovery of the HP-RDWC process via the
 109 ORC system is displayed in Figure 1. In this work, the proposed approach is conducted in
 110 three steps:

- 111 (1) The existing HP-RDWC process for the diethyl carbonate (DEC) process is simulated as
 112 the base case.
- 113 (2) An alternative configuration for the DEC production is proposed to recover waste heat via
 114 the ORC system.
- 115 (3) Five alternative working fluids are selected for the ORC system.
- 116 (4) The improved genetic algorithm is adopted to optimize the ORC system by using multiple
 117 objectives of net revenue and ORC efficiency.

118 In this section, simulation of the existing HP-RDWC in the first step is necessary.
 119 Temperature and heat duty of the heat source could be obtained, which could be used to

120 determine the proposed ORC assisted HP-RDWC configuration in step 2 and to select
 121 working fluid in step 3. Optimal design parameters of ORC system in step 4 are obtained via
 122 the improved genetic algorithm based on the results in steps 2 and 3.

123 **2.1 Existing heat pump assisted reactive dividing wall column process**

124 According to our previous study [16], the DEC production could be produced by the
 125 liquid catalytic reactions in the reactive section of the left side in the RDWC involving
 126 dimethyl carbonate (DMC), ethyl-methyl carbonate (EMC), ethanol (EtOH), and methanol
 127 (MeOH) as follows,



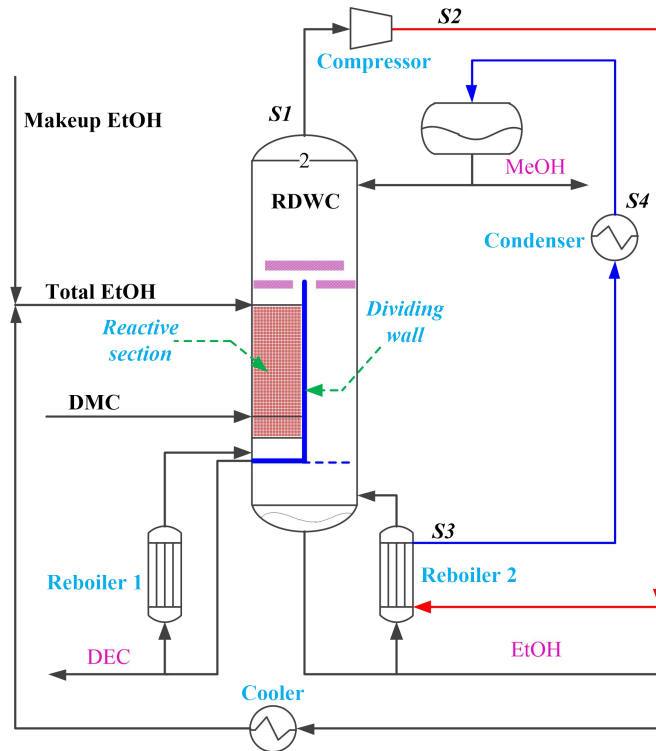
130 An experimental study on the chemical equilibrium and reaction kinetics of the DEC
 131 reaction system in a reactive distillation column is investigated by Keller et al. [42]. An
 132 improved investigated is studied to produce the DEC production via the catalyst sodium
 133 ethoxide as demonstrated in Eqs. 3-4.

$$134 \quad r_1 = x_{\text{cat}} \times (k_{f1} e^{-E_{f1}/RT} \alpha_{\text{DMC}} \alpha_{\text{EtOH}} - k_{b1} e^{-E_{b1}/RT} \alpha_{\text{EMC}} \alpha_{\text{MeOH}}) \quad (3)$$

$$135 \quad r_2 = x_{\text{cat}} \times (k_{f2} e^{-E_{f2}/RT} \alpha_{\text{EMC}} \alpha_{\text{EtOH}} - k_{b2} e^{-E_{b2}/RT} \alpha_{\text{DEC}} \alpha_{\text{MeOH}}) \quad (4)$$

136 where r_1 and r_2 are the reaction rate of Eqs. 1-2; the x_{cat} is the molar fraction of the catalyst.
 137 The temperature in K and the ideal gas constant in J/mol/K demonstrate as T and R ,
 138 respectively. The liquid activity of component x is expressed as α_x . The values of above
 139 mentioned parameters in Eqs. 3-4 are listed in the Table A1. In this work, the thermodynamic
 140 model UNIQUAC is selected to predict the vapor-liquid equilibrium. To establish the validity
 141 of the thermodynamic model used for this system, corresponding values of the coefficient of

142 determination (R^2) for all binary parameters are introduced. In addition, the built-in,
 143 regressing interaction parameters, and value of R^2 are displayed in Table A2.



144

145

Figure 2. Existing HP-RDWC scheme for producing DEC

146

147

148

149

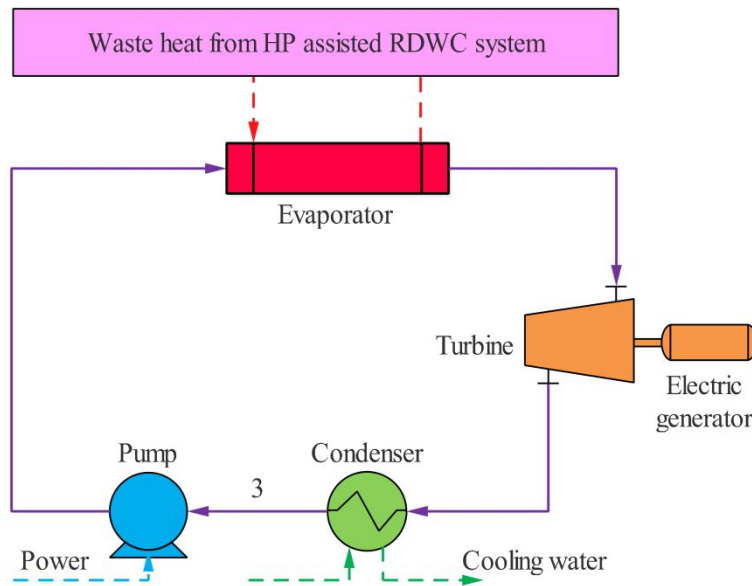
150

151

152

Zheng et al. [11] explored the synthesis of DEC via the reactive distillation and RDWC processes. Then, an energy-saving HP-RDWC process for the synthesis of DEC is reported by Yang et al. [16] as displayed in Figure 2. Feed flowrate, product purity, and feed composition of the existing HP-RDWC and the proposed process are consistent with the study of Zheng et al. [11]. The top vapor stream of the RDWC is compressed to heat the right reboiler 2 and it is then cooled via the condenser.

2.2 Conceptual design of the proposed alternative configurations



153

154

Figure 3. Scheme of waste heat recovery for HP-RDWC via the ORC system

155

156

157

158

Large amount of low-temperature ($<100\text{ }^{\circ}\text{C}$) waste heat is produced because the HP technique is used in the RDWC process. Hence, the ORC approach is used to effectively recover the low-temperature waste heat. The conceptual design of the proposed process is displayed in Figure 3.

159

2.3 Selection of working fluids

160

161

162

163

164

165

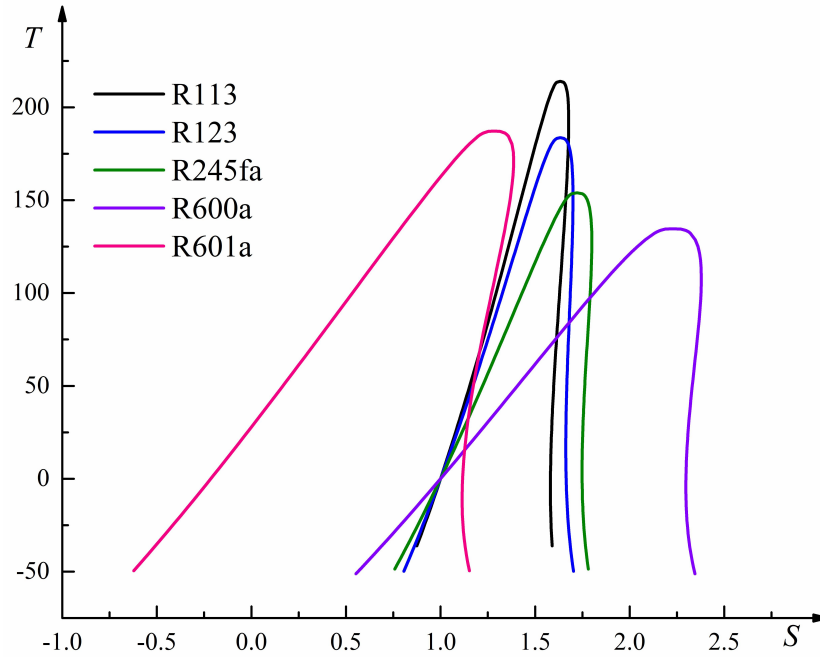
166

167

168

To obtain an ORC with best performance, the selection of the working fluids is a crucial step [43, 44]. Dry working fluids should be firstly determined based on the slope of saturation vapor line in the T-S diagram with positive because it has a higher thermodynamic efficiency [45]. Then, the critical temperature of the working fluid should be higher than that of heat source. If the critical temperature is closer to the heat source temperature, the thermodynamic efficiency is higher [43]. It is noteworthy that it is impossible to judge the economic performance directly from a single thermo-physical property. Other important thermo-physical properties (e.g., vaporization heat and environmental impacts) also should be considered in the selecting of working fluids [46]. Finally, the economic performance of

169 different working fluids should be obtained via the process optimization.



170

171

Figure 4. T-S diagram of five working fluids

172

Table 1. Properties of five organic working fluids studied in this work

Working fluid	R113	R123	R245fa	R600a	R601a
Chemical formula	CCl ₂ FCClF ₂	CF ₃ CHCl ₂	CF ₃ CH ₂ CHF ₂	C ₄ H ₁₀	C ₅ H ₁₂
CAS No.	76-13-1	306-83-2	460-73-1	75-28-5	78-78-4
Boiling point/°C	47.60	27.80	17.10	-11.70	27.80
Critical temperature/°C	214.10	183.70	154.00	134.70	187.80
Critical pressure/atm	33.65	36.12	36.02	36.02	32.86
Vaporization heat/kJ·kg ⁻¹	143.11	169.90	195.66	364.29	341.36
ODP	^a 0.85	^a 0.01	^a 0.00	^b 0.00	^b 0.00
GWP (100 y)	^a 6,130	^a 77.00	^a 1,050	^b 20.00	^b 20.00

173 Note: ^areference [47] and ^breferences [33, 48, 49].

174 Five working fluids candidates including R113, R123, R245fa, R600a, and R601a are

175 chosen to the ORC system. In addition, chemical formula, CAS No., boiling point, critical

176 temperature, critical pressure, vaporization heat, ozone destruction potential (ODP), and

177 global warming potential (GWP) are illustrated in Table 1 [22]. T-S diagram of five working

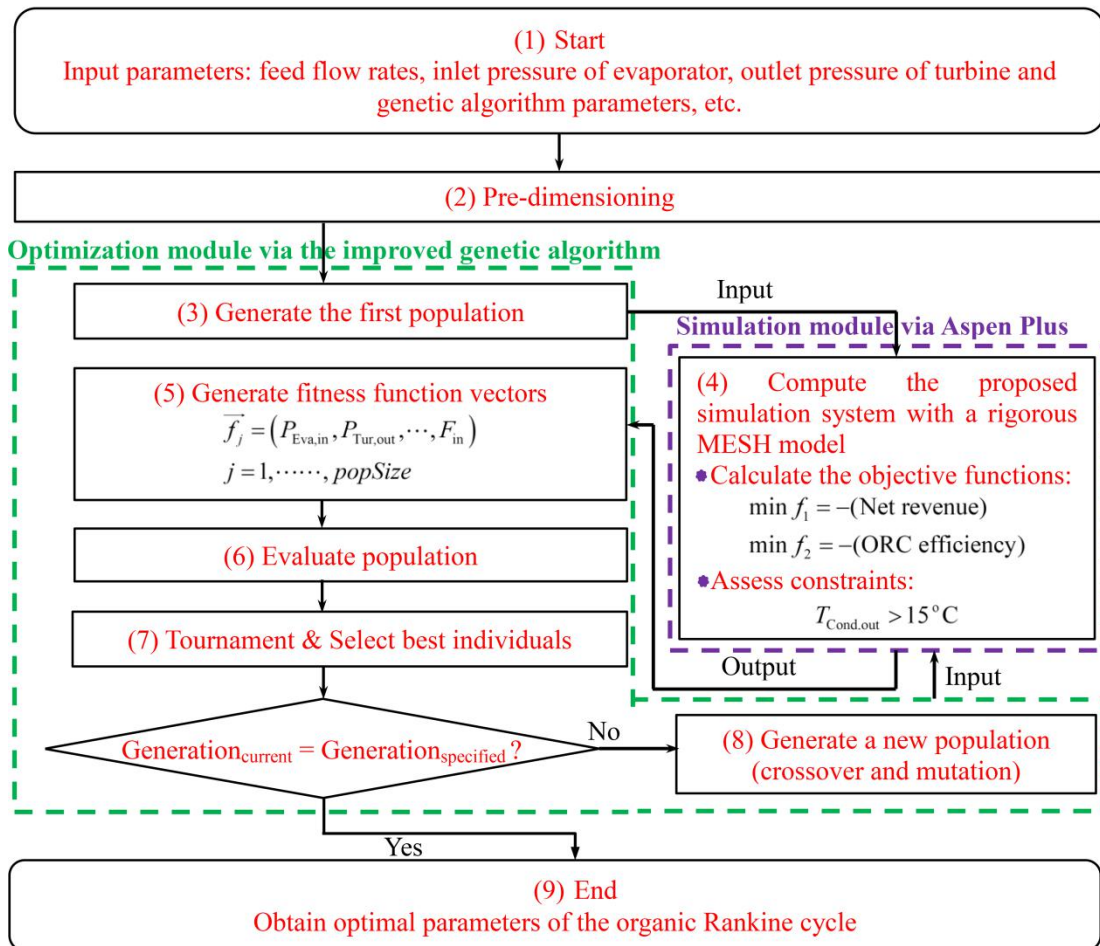
178 fluids is displayed in Figure 4.

179 2.4 Multi-objective optimization

180 In the optimization process, the improved genetic algorithm is adopted to optimize the
 181 ORC system by using net revenue and ORC efficiency as objectives (see Eqs. 5 and 6).

182 $\max f_1 = \text{Net revenue}$ (5)

183 $\max f_2 = \text{ORC thermal efficiency}$ (6)



184
 185 **Figure 5.** Scheme of the improved genetic algorithm for the organic Rankine cycle

186 The optimization approach combining the genetic algorithm and Aspen Plus is
 187 illustrated in Figure 5. In the optimization, the input parameters (e.g., feed flow rate) in step 1
 188 and pre-dimensioning in step 2 are firstly determined to import the optimization module. The
 189 first population generated by the improved genetic algorithm in step 3 as input is sent to step
 190 4 (Simulation module via Aspen Plus). Fitness function vectors are then generated in step 5
 191 via the calculation of objective functions and constraints in step 4. Evaluation of population is

192 realized in step 6. To reduce the repeated solutions and increase evolution rate, the step 7
 193 involving tournament & select best individuals is added. Is the current generation equal to the
 194 specified generation? If yes, the optimal parameters of the ORC are obtained in step 9.
 195 Otherwise, a new population is returned to step 4 via the crossover and mutation in step 8.

196 Initial population, evaluation population, tournament & select best individuals, and
 197 generation of new population are carried out in the improved genetic algorithm software
 198 while the corresponding parameters are listed in Table 2. A rigorous MESH (Mass balance
 199 equations, Equilibrium equations, Summation of mole fraction equations, and Heat or
 200 enthalpy balance equations) model of the proposed ORC scheme, calculation of objective
 201 functions, and evaluation of constraints are carried out in the Aspen Plus. The two conflicting
 202 objectives net revenue and ORC efficiency are used to optimize the ORC system (see step 4
 203 in Figure 5). Of note is that, improved genetic algorithm with a step 7 (i.e., tournament &
 204 select best individuals) is proposed to reduce the repeated solutions and increase evolution
 205 rate.

206 **Table 2.** Parameters of the multi-objective genetic algorithm used in the optimization process

Operator	Method	Parameter
Population size	-	<i>popSize</i> = 100
Restriction handle method	Dominance based method	<i>Niching</i> = yes
Selection method	Binary tournament	Tournament size = 2
Stopping criteria	Maximum number of generations	MaxGen
Crossover operator	SBX	-
Crossover probability	-	0.95
Mutation operator	Polynomial	-
Mutation probability	-	0.1

207 2.4.1 Net revenue

208 In this work, total capital cost involves the fixed investment of two heat exchangers and
 209 a turbine while the total energy investment includes the cost of electricity and cooling water.

210 Heat transfer area (A in m^2), capital cost of heat exchanger and turbine, energy cost of
 211 cooling water are illustrated in Eqs. 7-10 [22].

$$212 \quad A = \frac{Q}{u \times \Delta T} \quad (7)$$

$$213 \quad \text{Capital cost of heat exchanger} = \left(\frac{M\&S}{280}\right) \times (101.3 \times A^{0.65}) \times (2.29 + F_C) = 9367.8A^{0.65} \quad (8)$$

$$214 \quad \text{Capital cost of turbine} = 1.5 \times (225 + 170 \times V_{\text{outlet}}) \quad (9)$$

$$215 \quad \text{Energy cost of cooling water} = 8000 \times PCW \times CCW \quad (10)$$

216 where 1,468.6 of Marshall and Swift cost index (M&S) is suggested by Shahandeh et al. [50];
 217 correction factor of the heat exchanger (F_C) is determined as 15.3 [51, 52]; V_{outlet} (m^3/s) is the
 218 outlet volumetric flow rate of the turbine; heat transfer coefficient, u , is 0.865 kW/K/m^2 for
 219 condenser while u is 0.568 kW/K/m^2 for reboiler [53, 54]; price of cooling water is denoted
 220 as PCW (PCW = $0.03 \text{ US\$/t}$) [55-57]; consumption of cooling water is represented as CCW.
 221 It is noted that the cost of pump is neglected.

222 The total expenditure, earnings of electricity, and net revenue for the ORC system are
 223 given in Eqs. 11-13, respectively [14].

$$224 \quad \text{Total expenditure} = (\text{capital cost of heat exchanger} + \text{capital cost of turbine} \\ + \text{energy cost of cooling water}) / \text{payback period} \quad (11)$$

$$225 \quad \text{Earnings of electricity} = 8000 \times PE \times GC \quad (12)$$

$$226 \quad \text{Net revenue} = \text{earnings of electric} - \text{total expenditure} \quad (13)$$

227 where PE is the price of electricity (PE = $0.1 \text{ US\$/kW}\cdot\text{h}$) [22]. The deference between
 228 electricity of turbine and pump is denoted as generation capacity (denoted as GC in kW/h).

229 2.4.2 ORC thermal efficiency

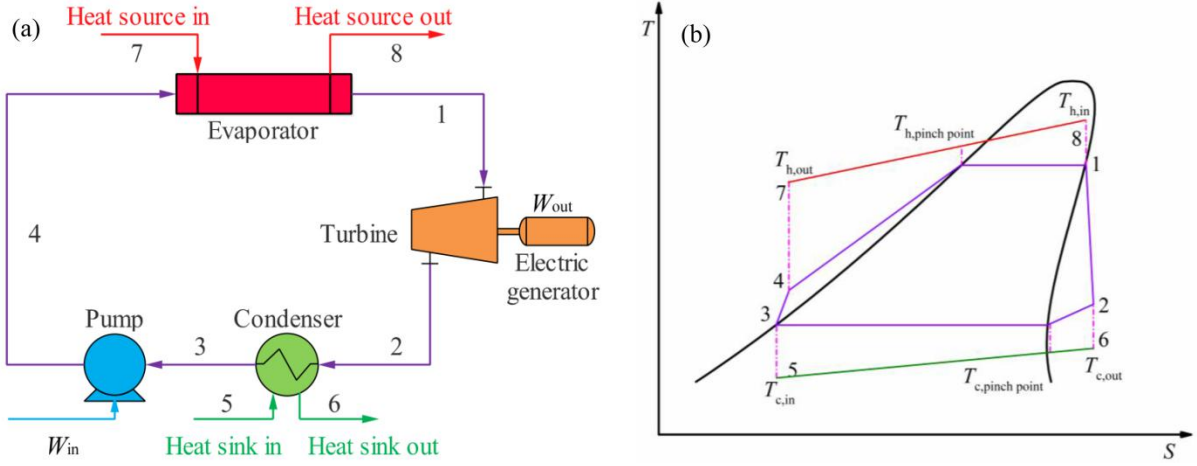


Figure 6. (a) Organic Rankine cycle system and (b) T-S diagram of the ORC system

Figure 6 illustrate the ORC and temperature-entropy (T-S) chart of the ORC system, respectively. As illustrated in Figure 6, four thermodynamic processes, isobaric heating (4→1) in the evaporator, isentropic expansion (1→2) in the turbine, isobaric cooling (2→3) in the condenser and isentropic compression (3→4) in the pump comprise the overall ORC system.

The ORC thermal efficiency is another important index, which could be calculated through the Eq. 14 [22, 23].

$$\text{ORC efficiency} = \frac{H_1 - H_2 - (H_3 - H_4)}{H_4 - H_1} \quad (14)$$

where H_3 and H_4 in kJ/kg are the enthalpy of working fluid at the inlet and outlet of pump; H_1 and H_2 in kJ/kg are the enthalpy of working fluid at the inlet and outlet of turbine.

2.4.3 Constraint

Following the study of Gao et al. [22], the outlet temperature of condenser ($T_{\text{Cond,out}}$) should be greater than 15 °C (see Eq. 15) to ensure that the working fluid at the condenser can be cooled by the cooling water.

$$T_{\text{Cond,out}} > 15^\circ\text{C} \quad (15)$$

2.4.4 Variables bounds

247 For the ORC system, four continuous variables as shown in Eqs. 16-19 involving flow
 248 rate of working fluid (F_{WF}), output pressure of the turbine ($P_{turbine}$), outlet pressure of the
 249 pump (P_{pump}), and the output temperature of the waste heat ($T_{WH,out}$) should be optimized.

$$250 \quad F_{WF}^{\min} \leq F_{WF} \leq F_{WF}^{\max} \quad (16)$$

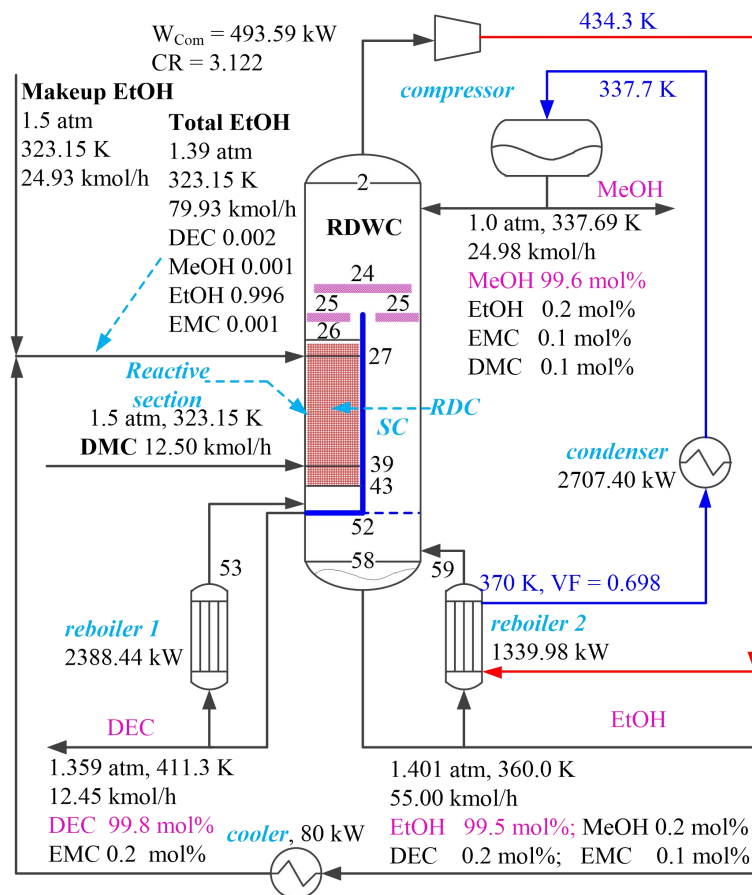
$$251 \quad P_{turbine}^{\min} \leq P_{turbine} \leq P_{turbine}^{\max} \quad (17)$$

$$252 \quad P_{pump}^{\min} \leq P_{pump} \leq P_{pump}^{\max} \quad (18)$$

$$253 \quad T_{WH,out}^{\min} \leq T_{WH,out} \leq T_{WH,out}^{\max} \quad (19)$$

254 3. Computational results and discussion

255 3.1 Simulation results of the existing HP-RDWC process



256

257

Figure 7. Simulation results of the existing HP-RDWC scheme

258

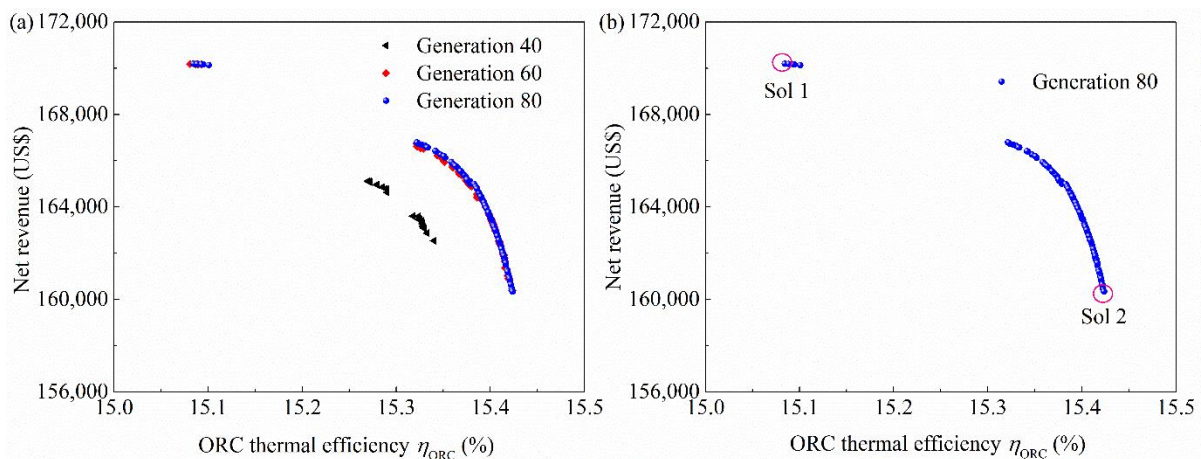
The reproduction of the existing HP-RDWC process for synthesis DEC is carried out in

259 Aspen Plus via two rigorous RadFrac models (see Figure A2). Figure 7 displays the
 260 simulation results of the existing HP-RDWC scheme. Product purities of DEC, EtOH, and
 261 MeOH are 99.8 mol%, 99.5 mol%, and 99.6 mol%, respectively. The vapour stream of the
 262 RDWC is compressed by the compressor to 3.14 atm with temperature increases to 434.3 K.
 263 In this process, the power of 493.59 kW is required to the compressor. The duty of the
 264 reboiler 2 is provided by the compressed stream. After that, the compressed stream with 370
 265 K is cooled to 337.7 K by using cooling water.

266 3.2 Optimization results

267 All design variables of ORC system are obtained via the improved genetic algorithm
 268 with net revenue and ORC efficiency as objective functions. The optimization is completed
 269 on the personal computer with Intel Core i7-7700 CPU@3.60GHZ, 8 GB memory. Lower
 270 and upper bounds of all design parameters and computational time are listed in Table A4.

271 3.2.1 ORC system with working fluid R113



272

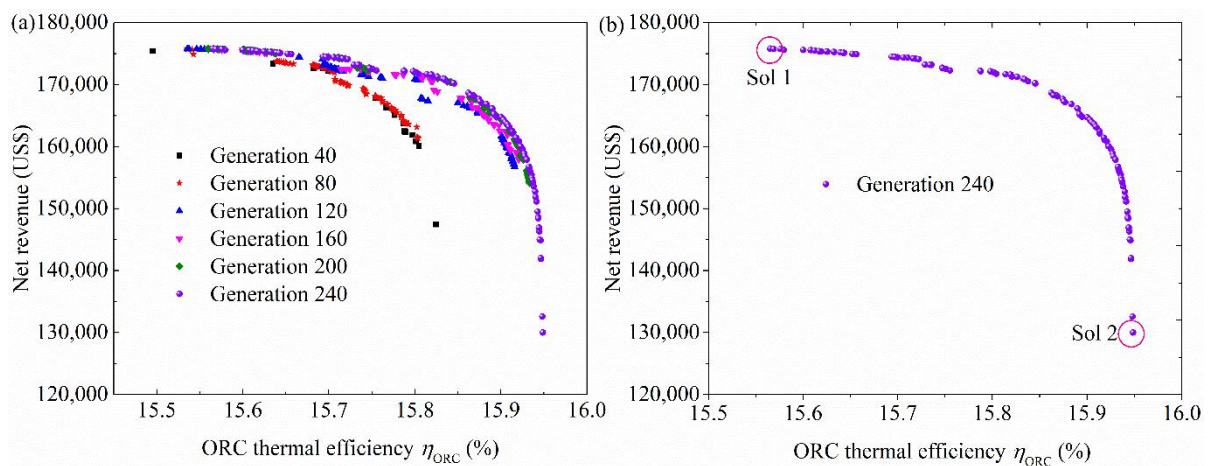
273 **Figure 8.** Multi-objective optimization (a) with different generations and (b) Pareto front
 274 solutions by using working fluid R113

275 An initial population of 100, crossover probability of 0.95, and mutation probability of

276 0.1 are used for the ORC system with working fluid R113. The optimization is terminated

277 after 80 generations by observing the vector of decision variables and it does not produce any
 278 meaningful improvement as illustrated in Figure 8a. The Pareto fronts between net revenue
 279 and ORC efficiency of 80 generations are shown in Figure 8b. There have two interesting
 280 solutions with highest net revenue solution (Sol 1) and highest ORC efficiency solution (Sol
 281 2).

282 3.2.2 ORC system with working fluid R123

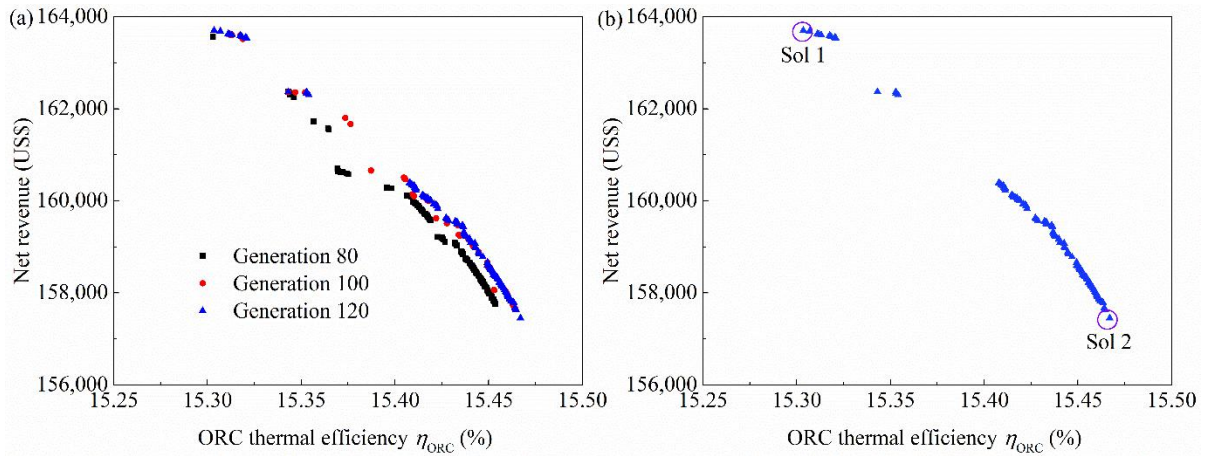


283

284 **Figure 9.** Multi-objective optimization (a) with different generations and (b) Pareto front
 285 solutions by using working fluid R123

286 The same settings (e.g., population and crossover strength) are used for the ORC system
 287 with working fluid R123. As illustrated in Figure 9a, very limited improvement in decision
 288 variables (i.e., net revenue and ORC thermal efficiency) can be seen from 200th to 240th
 289 generations indicating that the optimization procedure could be terminated after 240
 290 generations. Pareto fronts between net revenue and ORC efficiency of 240 generations are
 291 shown in Figure 9b. Two alternative solutions Sol 1 and Sol 2 (i.e., best economic and
 292 thermodynamic efficiency) are displayed in Figure 9b.

293 3.2.3 ORC system with working fluid R245fa

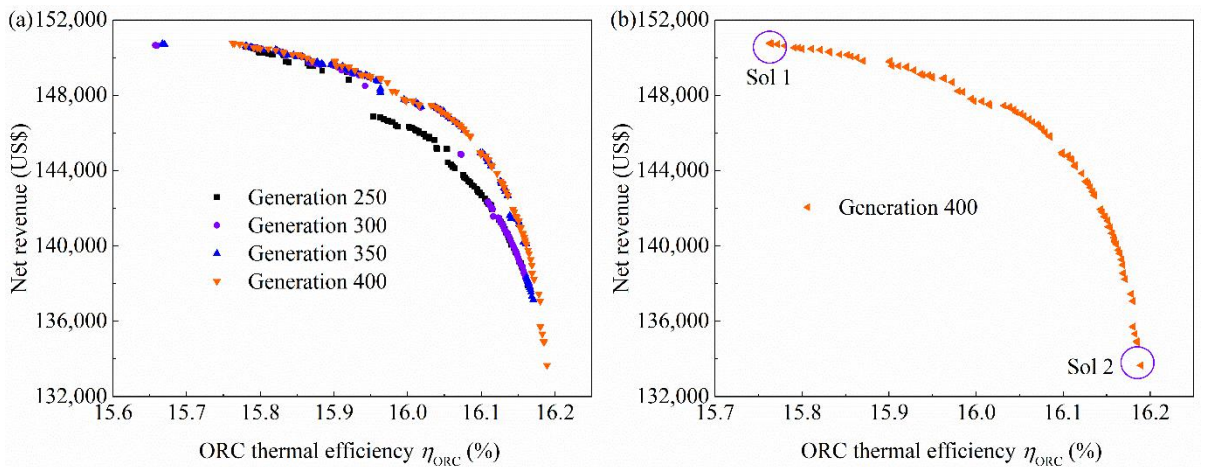


294

295 **Figure 10.** Multi-objective optimization (a) with different generations and (b) Pareto front
 296 solutions by using working fluid R245fa

297 Figure 10 displays the optimization results of the ORC system with working fluid
 298 R245fa. The trend of different generation and the optimal Pareto fronts between net revenue
 299 and ORC efficiency of 120 generations are shown in Figure 10a-b.

300 3.2.4 ORC system with working fluid R600a



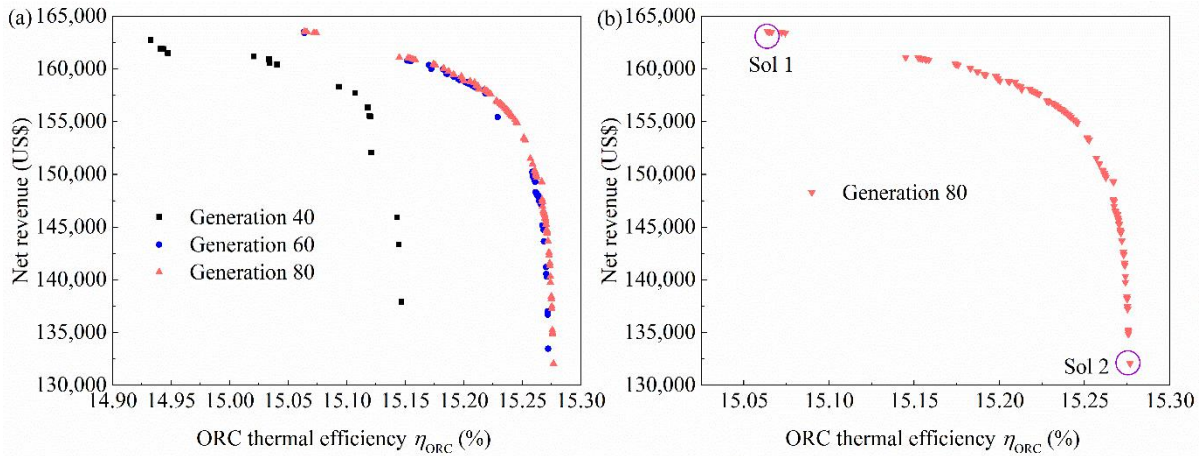
301

302 **Figure 11.** Multi-objective optimization (a) with different generations and (b) Pareto front
 303 solutions by using working fluid R600a

304 From the observation of multi-objective optimization with different generations as
 305 shown in Figure 11a, the optimization is terminated at 400 generations. The Pareto chart of
 306 ORC system with working fluid R600a is illustrated in Figure 11b, the values of the net
 307 revenue for this working fluid range from US\$ 132,000 to 152,000, whereas the ORC thermal

308 efficiency values obtained were in the range from 15.7% to 16.2%. Best net revenue design
 309 Sol 1 and best ORC thermal efficiency design Sol 2 are displayed in Figure 11b.

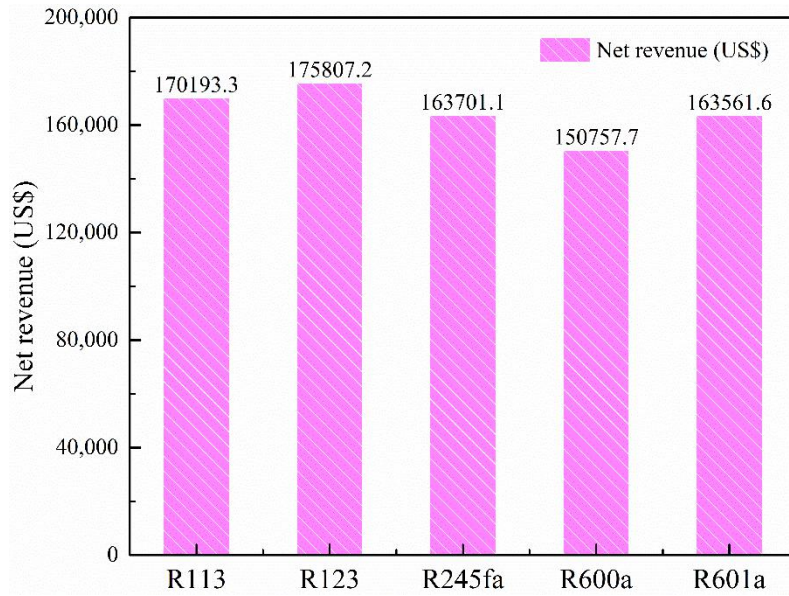
310 **3.2.5 ORC system with working fluid R601a**



311
 312 **Figure 12.** Multi-objective optimization (a) with different generations and (b) Pareto front
 313 solutions by using working fluid R601a

314 The settings of initial population, crossover probability, and mutation probability for the
 315 optimization of the ORC system with working fluid R601a are consistent with the settings of
 316 the working fluid R113. The multi-objective optimization of 40, 60, and 80 generations and
 317 the Pareto front of 80 generations are displayed in Figure 12a-b, respectively. In the same way,
 318 two representative optimized points are selected, Sol1 and Sol 2, the design variables of these
 319 designs are demonstrated in Figure 12b.

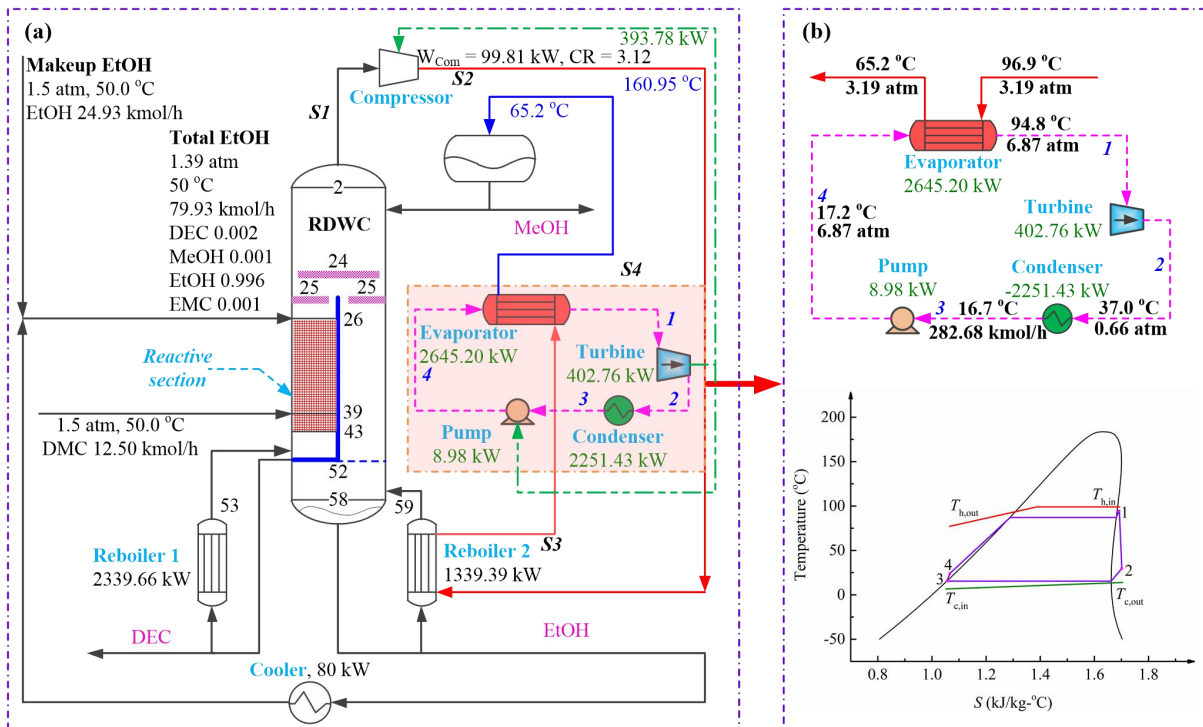
320 **3.3 Discussion and comparison**



321

322

Figure 13. Net revenue comparison of the ORC scheme by using five working fluids



323

324

325

Figure 14. The optimal ORC coupled with HP-RDWC scheme by using working fluid R123

326

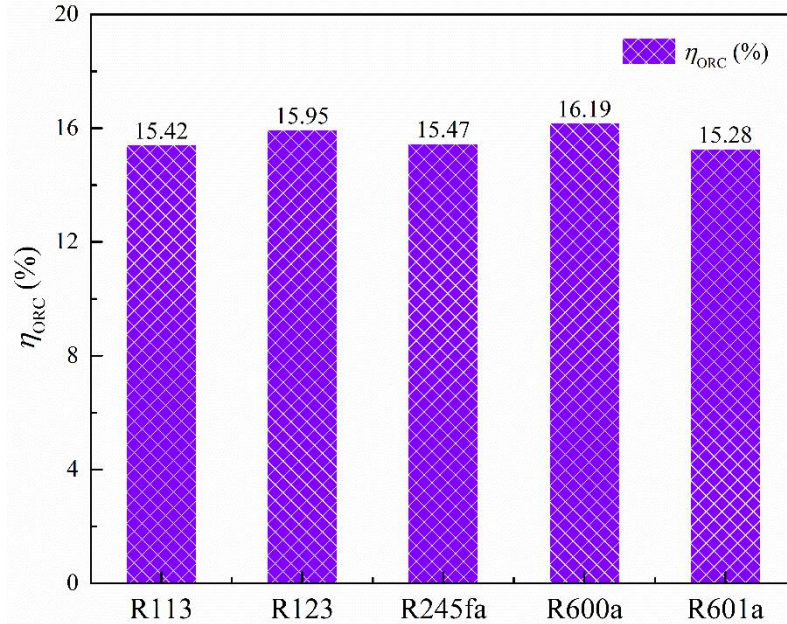
327

328

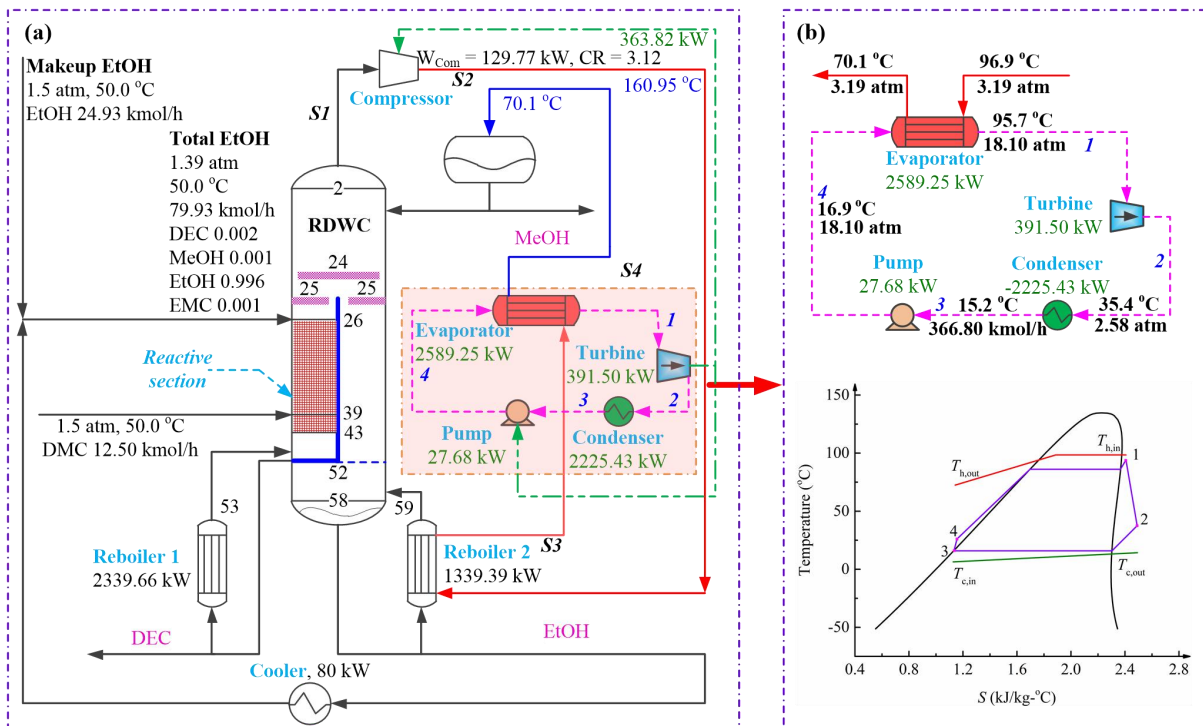
329

Figure 13 gives the net revenue comparison of the proposed ORC scheme by using five working fluids. The ORC system with working fluid R123 shows the best performance in the net revenue. The corresponding optimal ORC coupled with HP-RDWC scheme by using working fluid R123 is shown in Figure 14. The auxiliary power of compressor is 99.81 kW

330 and the 393.78 kW is provided by the ORC system. In summary, the per year net revenue
 331 (removing equipment costs of the ORC system) 175,807.2 US\$/y of the HP-RDWC process
 332 can be improved by using the ORC system.



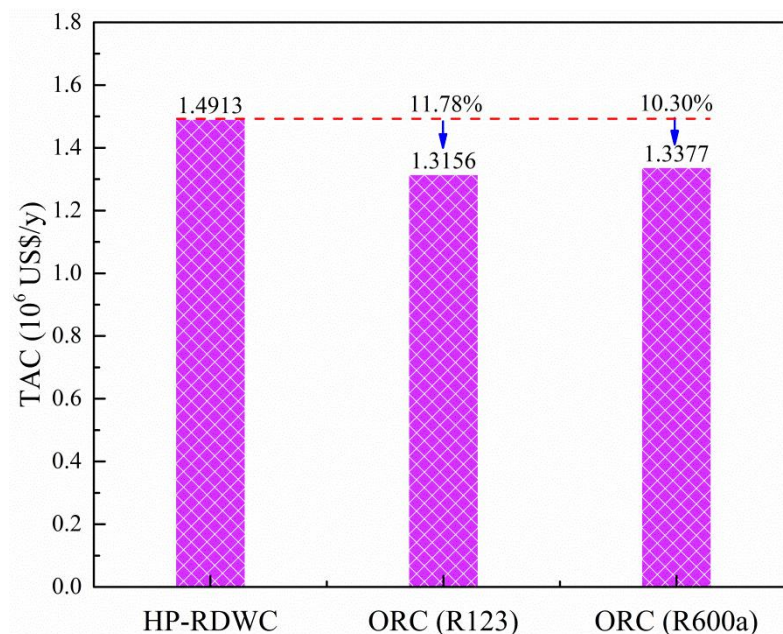
333
 334 **Figure 15.** ORC efficiency comparison of the ORC scheme by using five working fluids
 335



336
 337 **Figure 16.** The optimal ORC coupled with HP-RDWC scheme by using working fluid R600a

338 The ORC thermal efficiency comparisons of five alternative working fluids are
 339 displayed in Figure 15. The ORC system with working fluid R600a has the best performance
 340 in the ORC thermal efficiency ($\eta_{ORC} = 16.19\%$). The HP-RDWC process combined with
 341 ORC system with detailed operating condition information is demonstrated in Figure 16. The
 342 amount power of 363.82 kW for the compressor could be provided by the ORC system while
 343 the auxiliary power of compressor is 129.77 kW. In summary, the per year net revenue
 344 (removing equipment costs of the ORC system) of the HP-RDWC process applying the ORC
 345 system can be improved by 133,664.5 US\$/y.

346 It can be seen from Figure 13, the working fluid R123 shows the best performance in
 347 economy while the ODP and GWP are slightly larger than the working fluid R600a. The
 348 results of Figure 15 demonstrated that the working fluid R600a has the highest
 349 thermodynamic efficiency, which is consistent with the description in Section 2.3. In addition,
 350 the working fluid R600a has the best performances in the environmentally friendly category
 351 because it has a lowest ODP and GEP.



352 **Figure 17.** Economic comparisons of the existing and proposed processes
 353

354 The detailed economic performances involving capital and energy costs of three designs
355 and each unit are displayed in Figure 17 and Table A5, respectively. TAC of the ORC assisted
356 HP-RDWC schemes with working fluids R123 and R600a are respectively reduced by
357 11.78% and 10.30%. In summary, economic benefit of the heat pump process could be
358 significantly improved via the ORC system.

359 **4. Conclusion**

360 A sustainable process of heat pump assisted reactive dividing wall column (HP-RDWC)
361 combined with organic Rankine cycle (ORC) is proposed for the synthesis of diethyl
362 carbonate. A great deal of low-temperature ($<100\text{ }^{\circ}\text{C}$) waste heat of the HP-RDWC process
363 has been demonstrated to be converted to the clean energy via the proposed ORC system.
364 Five safer, greener, and dry working fluids are determined to the ORC system. The ORC
365 system with the best performance is optimized using the improved genetic algorithm while
366 taking both net revenue and ORC thermal efficiency as objectives. The optimizations
367 illustrated that the net output power of 393.78 kW, the net revenue of 175,807.2 US\$/y, and
368 ORC efficiency of 15.57% could be produced via adding the ORC system with working fluid
369 R123. Net output power of 363.82 kW, net revenue of 133,665.5 US\$/y, and ORC efficiency
370 of 16.19% could be achieved via adding the ORC assisted HP-RDWC with working fluid
371 R600a. Compared with the existing HP-RDWC process, HP-RDWC integrated ORC scheme
372 with working fluids R123 and R600a can save 11.78% and 10.30% of total annual cost,
373 respectively. It is noted that the proposed approach could be extended to other heat pump or
374 overall plant systems to produce clean energy.

375 **Acknowledgments**

376 We acknowledge the financial support provided by the Fundamental Research Funds for the
377 Central Universities (Nos. 2019CDXYHG0012, 2019CDQYHG021); the National Natural
378 Science Foundation of China (Nos. 21606026, 21878028); the Chongqing Innovation Support
379 Program for Returned Overseas Chinese Scholars (No. CX2018048). We are also grateful
380 to the comments from the anonymous reviewer.

381 **Nomenclature**

382	DWC	dividing wall column
383	HP	heat pump
384	ORC	organic Rankine cycle
385	TAC	total annual cost
386	RDWC	reactive dividing wall column
387	η_{ORC}	ORC thermal efficiency
388	HP-RDWC	heat pump-reactive dividing wall column
389	DEC	diethyl carbonate
390	EMC	ethyl-methyl carbonate
391	DMC	dimethyl carbonate
392	ethanol	EtOH
393	methanol	MeOH
394	r_i	reaction rate of the reaction i
395	k_{fi}	forward pre-exponential factors of the reaction i
396	k_{bi}	backward pre-exponential factors of the reaction i
397	E_{fi}	forward activation energies of the reaction i , kJ/kmol

398 E_{bi} backward activation energies of the reaction i , kJ/kmol

399 H enthalpy, kW

400 S entropy, kJ/(kg·K)

401 GWP global warning potential

402 ODP ozone destruction potential

403 **References**

404 [1] Ren J, Sovacool BK. Enhancing China's energy security: Determining influential factors
405 and effective strategic measures. *Energ Convers Manage* 2014;88:589-97.

406 <https://doi.org/10.1016/j.enconman.2014.09.001>

407 [2] Ren J, Sovacool BK. Prioritizing low-carbon energy sources to enhance China's energy
408 security. *Energ Convers Manage* 2015;92:129-36.

409 <https://doi.org/10.1016/j.enconman.2014.12.044>

410 [3] Petlyuk FB, Platonov VM, Slavinskii DM. Thermodynamically optimal method for
411 separating multicomponent mixtures. *Int Chem Eng* 1965;5(3):555-61.

412 [4] Dejanović I, Matijašević L, Olujić Ž. Dividing wall column—a breakthrough towards
413 sustainable distilling. *Chem Eng Process* 2010;49(6):559-80.

414 <https://doi.org/10.1016/j.cep.2010.04.001>

415 [5] Benyounes H, Benyahia K, Shen W, Gerbaud V, Dong L, Wei S. Novel Procedure for
416 Assessment of Feasible Design Parameters of Dividing-Wall Columns: Application to
417 Non-azeotropic Mixtures. *Ind Eng Chem Res* 2015;54(19):5307-18.

418 <https://doi.org/10.1021/ie5048576>

419 [6] Seihoub F-Z, Benyounes H, Shen W, Gerbaud V. An Improved Shortcut Design Method

420 of Divided Wall Columns Exemplified by a Liquefied Petroleum Gas Process. *Ind Eng Chem*
421 *Res* 2017;56(34):9710-20. <https://doi.org/10.1021/acs.iecr.7b02125>

422 [7] Long H, Clark J, Benyounes H, Shen W, Dong L, Wei S. Optimal Design and Economic
423 Evaluation of Dividing-Wall Columns. *Chem Eng Technol* 2016;39(6):1077-86.
424 <https://doi.org/10.1002/ceat.201500106>

425 [8] Premkumar R, Rangaiah GP. Retrofitting conventional column systems to dividing-Wall
426 Columns. *Chem Eng Res Des* 2009;87(1):47-60. <https://doi.org/10.1016/j.cherd.2008.06.013>

427 [9] Kiss AA, Segovia-Hernández JG, Bildea CS, Miranda-Galindo EY, Hernández S.
428 Reactive DWC leading the way to FAME and fortune. *Fuel* 2012;95:352-9.
429 <https://doi.org/10.1016/j.fuel.2011.12.064>

430 [10] Yang A, Lv L, Shen W, Dong L, Li J, Xiao X. Optimal Design and Effective Control of
431 the tert-Amyl Methyl Ether Production Process Using an Integrated Reactive Dividing Wall
432 and Pressure Swing Columns. *Ind Eng Chem Res* 2017;56(49):14565-81.
433 <https://doi.org/10.1021/acs.iecr.7b03459>

434 [11] Zheng L, Cai W, Zhang X, Wang Y. Design and control of reactive dividing-wall column
435 for the synthesis of diethyl carbonate. *Chem Eng Process* 2017;111:127-40.
436 <https://doi.org/10.1016/j.cep.2016.09.014>

437 [12] Li L, Sun L, Yang D, Zhong W, Zhu Y, Tian Y. Reactive dividing wall column for
438 hydrolysis of methyl acetate: Design and control. *Chin J Chem Eng* 2016;24(10):1360-8.
439 <https://doi.org/10.1016/j.cjche.2016.05.023>

440 [13] Sun S, Yang A, Chien IL, Shen W, Wei S, Ren J, Zhang X. Intensification and
441 performance assessment for synthesis of 2-methoxy-2-methyl-heptane through the combined

442 use of different pressure thermally coupled reactive distillation and heat integration technique.
443 Chem Eng Process 2019;142:107561. <https://doi.org/10.1016/j.cep.2019.107561>

444 [14] Yang A, Jin S, Shen W, Cui P, Chien IL, Ren J. Investigation of energy-saving azeotropic
445 dividing wall column to achieve cleaner production via heat exchanger network and heat
446 pump technique. J Clean Prod 2019;234:410-22. <https://doi.org/10.1016/j.jclepro.2019.06.224>

447 [15] Feng S, Ye Q, Xia H, Li R, Suo X. Integrating a vapor recompression heat pump into a
448 lower partitioned reactive dividing-wall column for better energy-saving performance. Chem
449 Eng Res Des 2017;125:204-13. <https://doi.org/10.1016/j.cherd.2017.07.017>

450 [16] Yang A, Sun S, Eslamimanesh A, Wei S, Shen W. Energy-saving investigation for diethyl
451 carbonate synthesis through the reactive dividing wall column combining the vapor
452 recompression heat pump or different pressure thermally coupled technique. Energy
453 2019;172:320-32. <https://doi.org/10.1016/j.energy.2019.01.126>

454 [17] Jang W, Lee H, Han J-i, Lee JW. Energy-Efficient Reactive Dividing Wall Column for
455 Simultaneous Esterification of n-Amyl Alcohol and n-Hexanol. Ind Eng Chem Res
456 2019;58(19):8206-19. <https://doi.org/10.1021/acs.iecr.9b00324>

457 [18] Feng Z, Shen W, Rangaiah GP, Lv L, Dong L. Process Development, Assessment, and
458 Control of Reactive Dividing-Wall Column with Vapor Recompression for Producing
459 n-Propyl Acetate. Ind Eng Chem Res 2018;58(1):276-95.
460 <https://doi.org/10.1021/acs.iecr.8b05122>

461 [19] Shi L, Wang SJ, Huang K, Wong DSH, Yuan Y, Chen H, Zhang L, Wang S. Intensifying
462 reactive dividing-wall distillation processes via vapor recompression heat pump. J Taiwan
463 Inst Chem E 2017;78:8-19. <https://doi.org/10.1016/j.jtice.2017.05.013>

464 [20] Suo X, Ye Q, Li R, Feng S, Xia H. Investigation about Energy Saving for Synthesis of
465 Isobutyl Acetate in the Reactive Dividing-Wall Column. *Ind Eng Chem Res*
466 2017;56(19):5607-17. <https://doi.org/10.1021/acs.iecr.6b04354>

467 [21] Quoilin S, Broek MVD, Declaye S, Dewallef P, Lemort V. Techno-economic survey of
468 Organic Rankine Cycle (ORC) systems. *Renew Sust Energ Rev* 2013;22:168-86.
469 <https://doi.org/10.1016/j.rser.2013.01.028>

470 [22] Gao X, Gu Q, Ma J, Zeng Y. MVR heat pump distillation coupled with ORC process for
471 separating a benzene-toluene mixture. *Energy*. 2018;143:658-65.
472 <https://doi.org/10.1016/j.energy.2017.11.041>

473 [23] Gao X, Yin X, Yang S, Yang D. Improved Organic Rankine Cycle System Coupled with
474 Mechanical Vapor Recompression Distillation for Separation of Benzene-Toluene Mixture.
475 *Process Integr Optim Sustain* 2019;3(2):189-98. <https://doi.org/10.1007/s41660-018-0076-8>

476 [24] Baccioli A, Antonelli M, Desideri U, Grossi A. Thermodynamic and economic analysis
477 of the integration of Organic Rankine Cycle and Multi-Effect Distillation in waste-heat
478 recovery applications. *Energy*. 2018;161:456-69. <https://doi.org/10.1016/j.energy.2018.07.150>

479 [25] Han F, Wang Z, Ji Y, Li W, Sundén B. Energy analysis and multi-objective optimization
480 of waste heat and cold energy recovery process in LNG-fueled vessels based on a triple
481 organic Rankine cycle. *Energ Convers Manage* 2019;195:561-72.
482 <https://doi.org/10.1016/j.enconman.2019.05.040>

483 [26] Hipólito-Valencia BJ, Rubio-Castro E, Ponce-Ortega JM, Serna-González M,
484 Nápoles-Rivera F, El-Halwagi MM. Optimal integration of organic Rankine cycles with
485 industrial processes. *Energ Convers Manage* 2013;73:285-302.

486 <https://doi.org/10.1016/j.enconman.2013.04.036>

487 [27] Hipólito-Valencia BgJ, Vázquez-Ojeda M, Segovia-Hernández JG, Ponce-Ortega JM.
488 Waste Heat Recovery through Organic Rankine Cycles in the Bioethanol Separation Process.
489 *Ind Eng Chem Res* 2014;53(16):6773-88. <https://doi.org/10.1021/ie404202a>

490 [28] Pili R, Romagnoli A, Jiménez-Arreola M, Spliethoff H, Wieland C. Simulation of
491 Organic Rankine Cycle–Quasi-steady state vs dynamic approach for optimal economic
492 performance. *Energy* 2019;167:619-40. <https://doi.org/10.1016/j.energy.2018.10.166>

493 [29] Liu X, Liang J, Xiang D, Yang S, Qian Y. A proposed coal-to-methanol process with
494 CO₂ capture combined Organic Rankine Cycle (ORC) for waste heat recovery. *J Clean Prod*
495 2016;129:53-64. <https://doi.org/10.1016/j.jclepro.2016.04.123>

496 [30] Zhang H, Guan X, Ding Y, Liu C. Emergy analysis of Organic Rankine Cycle (ORC) for
497 waste heat power generation. *J Clean Prod* 2018;183:1207-15.
498 <https://doi.org/10.1016/j.jclepro.2018.02.170>

499 [31] Yağlı H, Koç Y, Koç A, Görgülü A, Tandiroğlu A. Parametric optimization and exergetic
500 analysis comparison of subcritical and supercritical organic Rankine cycle (ORC) for biogas
501 fuelled combined heat and power (CHP) engine exhaust gas waste heat. *Energy*
502 2016;111:923-32. <https://doi.org/10.1016/j.energy.2016.05.119>

503 [32] Baldasso E, Andreasen JG, Mondejar ME, Larsen U, Haglind F. Technical and economic
504 feasibility of organic Rankine cycle-based waste heat recovery systems on feeder ships:
505 Impact of nitrogen oxides emission abatement technologies. *Energy Convers Manage*
506 2019;183:577-89. <https://doi.org/10.1016/j.enconman.2018.12.114>

507 [33] Li J, Duan Y, Yang Z, Yang F. Exergy analysis of novel dual-pressure evaporation

508 organic Rankine cycle using zeotropic mixtures. *Energ Convers Manage* 2019;195:760-9.
509 <https://doi.org/10.1016/j.enconman.2019.05.052>

510 [34] Li P, Han Z, Jia X, Mei Z, Han X, Wang Z. Comparative analysis of an organic Rankine
511 cycle with different turbine efficiency models based on multi-objective optimization. *Energ*
512 *Convers Manage* 2019;185:130-42. <https://doi.org/10.1016/j.enconman.2019.01.117>

513 [35] Li T, Meng N, Liu J, Zhu J, Kong X. Thermodynamic and economic evaluation of the
514 organic Rankine cycle (ORC) and two-stage series organic Rankine cycle (TSORC) for flue
515 gas heat recovery. *Energ Convers Manage* 2019;183:816-29.
516 <https://doi.org/10.1016/j.enconman.2018.12.094>

517 [36] Mohammadi K, McGowan JG. Thermoeconomic analysis of multi-stage recuperative
518 Brayton cycles: Part II – Waste energy recovery using CO₂ and organic Rankine power
519 cycles. *Energ Convers Manage* 2019;185:920-34.
520 <https://doi.org/10.1016/j.enconman.2019.01.091>

521 [37] Yagli H, Koc A, Karakus C, Koc Y. Comparison of toluene and cyclohexane as a
522 working fluid of an organic Rankine cycle used for reheat furnace waste heat recovery. *Int J*
523 *Exergy*. 2016;19(3):420-38. <https://doi.org/10.1504/IJEX.2016.075677>

524 [38] Koç Y, Yağlı H, Koç A. Exergy Analysis and Performance Improvement of a
525 Subcritical/Supercritical Organic Rankine Cycle (ORC) for Exhaust Gas Waste Heat
526 Recovery in a Biogas Fuelled Combined Heat and Power (CHP) Engine Through the Use of
527 Regeneration. *Energies* 2019;12(4). <https://www.mdpi.com/1996-1073/12/4/575/pdf>

528 [39] Zhi L-H, Hu P, Chen LX, Zhao G. Parametric analysis and optimization of
529 transcritical-subcritical dual-loop organic Rankine cycle using zeotropic mixtures for engine

530 waste heat recovery. *Energ Convers Manage* 2019;195:770-87.
531 <https://doi.org/10.1016/j.enconman.2019.05.062>

532 [40] Holik M, Živić M, Virag Z, Barac A. Optimization of an organic Rankine cycle
533 constrained by the application of compact heat exchangers. *Energ Convers Manage*
534 2019;188:333-45. <https://doi.org/10.1016/j.enconman.2019.03.039>

535 [41] Li X, Cui C, Li H, Gao X. Process synthesis and simultaneous optimization of extractive
536 distillation system integrated with organic Rankine cycle and economizer for waste heat
537 recovery. *J Taiwan Inst Chem E* 2019;102:61-72. <https://doi.org/10.1016/j.jtice.2019.07.003>

538 [42] Keller T, Holtbruegge J, Niesbach A, Górak A. Transesterification of Dimethyl
539 Carbonate with Ethanol To Form Ethyl Methyl Carbonate and Diethyl Carbonate: A
540 Comprehensive Study on Chemical Equilibrium and Reaction Kinetics. *Ind Eng Chem Res*
541 2011;50(19):11073-86. <https://pubs.acs.org/doi/10.1021/ie2014982>

542 [43] Kajurek J, Rusowicz A, Grzebielec A, Bujalski W, Futyma K, Rudowicz Z. Selection of
543 refrigerants for a modified organic Rankine cycle. *Energy* 2019;168:1-8.
544 <https://doi.org/10.1016/j.energy.2018.11.024>

545 [44] Saleh B, Koglbauer G, Wendland M, Fischer J. Working fluids for low-temperature
546 organic Rankine cycles. *Energy* 2007;32(7):1210-21.
547 <https://doi.org/10.1016/j.energy.2006.07.001>

548 [45] Bao J, Zhao L. A review of working fluid and expander selections for organic Rankine
549 cycle. *Renew Sust Energ Rev* 2013;24:325-42. <https://doi.org/10.1016/j.rser.2013.03.040>

550 [46] Tchanche BF, Papadakis G, Lambrinos G, Frangoudakis A. Fluid selection for a
551 low-temperature solar organic Rankine cycle. *Appl Therm Eng* 2009;29(11-12):2468-76.

552 <https://doi.org/10.1016/j.applthermaleng.2008.12.025>

553 [47] Besagni G, Mereu R, Inzoli F. Ejector refrigeration: A comprehensive review. *Renew*
554 *Sust Energ Rev* 2016;53:373-407. <https://doi.org/10.1016/j.rser.2015.08.059>

555 [48] Li J, Ge Z, Duan Y, Yang Z. Performance analyses and improvement guidelines for
556 organic Rankine cycles using R600a/R601a mixtures driven by heat sources of 100°C to
557 200°C. *Int J Energ Res* 2019;43(2):905-20. <https://doi.org/10.1002/er.4324>

558 [49] Nematollahi O, Hajabdollahi Z, Hoghooghi H, Kim KC. An evaluation of wind turbine
559 waste heat recovery using organic Rankine cycle. *J Clean Prod* 2019;214:705-16.
560 <https://doi.org/10.1016/j.jclepro.2019.01.009>

561 [50] Shahandeh H, Jafari M, Kasiri N, Ivakpour J. Economic optimization of heat
562 pump-assisted distillation columns in methanol-water separation. *Energy* 2015;80:496-508.
563 <https://doi.org/10.1016/j.energy.2014.12.006>

564 [51] Yang A, Su Y, Chien IL, Jin S, Yan C, Wei S, Shen W. Investigation of an energy-saving
565 double-thermally coupled extractive distillation for separating ternary system
566 benzene/toluene/cyclohexane. *Energy* 2019;186:115756.
567 <https://doi.org/10.1016/j.energy.2019.07.086>

568 [52] Yang A, Sun S, Shi T, Xu D, Ren J, Shen W. Energy-efficient extractive pressure-swing
569 distillation for separating binary minimum azeotropic mixture dimethyl carbonate and ethanol.
570 *Sep Purifi Technol* 2019;229:115817. <https://doi.org/10.1016/j.seppur.2019.115817>

571 [53] Wang C, Guang C, Cui Y, Wang C, Zhang Z. Compared novel thermally coupled
572 extractive distillation sequences for separating multi-azeotropic mixture of
573 acetonitrile/benzene/methanol. *Chem Eng Res Des* 2018;136:513-28.

574 <https://doi.org/10.1016/j.cherd.2018.06.017>

575 [54] Yang A, Wei R, Sun S, Wei S, Shen W, Chien IL. Energy-Saving Optimal Design and
576 Effective Control of Heat Integration-Extractive Dividing Wall Column for Separating
577 Heterogeneous Mixture Methanol/Toluene/Water with Multiazeotropes. *Ind Eng Chem Res*
578 2018;57(23):8036-56. <https://pubs.acs.org/doi/10.1021/acs.iecr.8b00668>

579 [55] Yang A, Shen W, Wei S, Dong L, Li J, Gerbaud V. Design and control of pressure-swing
580 distillation for separating ternary systems with three binary minimum azeotropes. *AIChE J*
581 2019;65(4):1281-93. <https://doi.org/10.1002/aic.16526>

582 [56] Shen W, Dong L, Wei S, Li J, Benyounes H, You X, Gerbaud V. Systematic design of an
583 extractive distillation for maximum-boiling azeotropes with heavy entrainers. *AIChE J*
584 2015;61(11):3898-910. <https://doi.org/10.1002/aic.14908>

585 [57] Shi T, Yang A, Jin S, Shen W, Wei S, Ren J. Comparative optimal design and control of
586 two alternative approaches for separating heterogeneous mixtures isopropyl alcohol-isopropyl
587 acetate-water with four azeotropes. *Sep Purifi Technol* 2019;225:1-17.
588 <https://doi.org/10.1016/j.seppur.2019.05.061>

589